

CHEMISTRY & SUSTAINABILITY

CHEM **SUS** CHEM

ENERGY & MATERIALS

Accepted Article

Title: Ternary Pt/Au/TiO₂-Decorated Plasmonic Wood Carbon for High-Efficiency Interfacial Solar Steam Generation and Photodegradation of Tetracycline

Authors: Minmin Wang, Ping Wang, Jie Zhang, Chuanping Li, and Yongdong Jin

This manuscript has been accepted after peer review and appears as an Accepted Article online prior to editing, proofing, and formal publication of the final Version of Record (VoR). This work is currently citable by using the Digital Object Identifier (DOI) given below. The VoR will be published online in Early View as soon as possible and may be different to this Accepted Article as a result of editing. Readers should obtain the VoR from the journal website shown below when it is published to ensure accuracy of information. The authors are responsible for the content of this Accepted Article.

To be cited as: *ChemSusChem* 10.1002/cssc.201802485

Link to VoR: <http://dx.doi.org/10.1002/cssc.201802485>

Ternary Pt/Au/TiO₂-Decorated Plasmonic Wood Carbon for High-Efficiency Interfacial Solar Steam Generation and Photodegradation of Tetracycline

Minmin Wang,^{[a],[b]} Ping Wang,^[a] Jie Zhang,^[a] Chuanping Li,^{[a],[b]} and Yongdong Jin*^{[a],[b]}

Abstract: A ternary Pt/Au/TiO₂ nanoparticles (NPs) decorated plasmonic wood carbon has been successfully fabricated by a simple two-step calcination method. The as-prepared Pt/Au/TiO₂ NPs-decorated wood carbon showed interfacial solar steam generation efficiency up to 90.4%. Meanwhile, the floating system exhibit excellent photodegradation rate of TC (at 40 mg L⁻¹) up to 94% after 80 min continuous light irradiation ($\lambda > 420$ nm) with the assistance of solar steam process which is superior to previously reported photocatalysts. The photocatalysis is promoted by the introduction of Pt/Au nanocomponents (which suppress the recombination of electron-hole pairs generated in TiO₂ and facilitate electron transfer). High-performance liquid chromatography-mass spectrometry (HPLC-MS) was employed to identify the photocatalytic reaction products of the system, and a mechanistic insight was also provided. The as-prepared 3D plasmonic wood carbon with high photocatalytic performance, rendering such wood-carbon based system recyclable and up-scalable for practical versatile solar-driven clean water generation.

Introduction

In recent years, effective solar energy conversion has been widely studied and used to relieve growing energy and environmental issues.^[1] Among various methods, photocatalytic oxidation technique based on semiconductors for environmental remediation has received much attentions. Titanium dioxide (TiO₂) is the most promising water treatment photocatalyst because of its good photocatalytic efficiency. Unfortunately, the small specific surface area and lacked visible light utilization limit its photocatalytic activity. In order to break these limitations, extensive research efforts have been focused on finding effective ways to improve its photocatalytic performance.^[2] Hybridizing photocatalysts by taking advantage of surface plasmon resonance of metal NPs was an effective way to increase visible light absorption of TiO₂.^[3] Meanwhile, finding effective photocatalyst carriers or promoters is another effective way to improve the photocatalytic activity of TiO₂. Carbonaceous materials such as activated carbon and carbon fibers with high specific surface area and pore volume have therefore been used as supports to load TiO₂, which resulting in excellent adsorption

capacity for pollutants. However, the activated carbon is not an economical adsorbent for its extra chemical or physical activation process. Therefore, it is necessary to develop cheap carbonaceous materials with simple preparation methods to combine TiO₂ to remove pollutants for the practical applications.

Wood carbon with numerous low tortuosity micro- and nano-channels seems to be a surprising candidate serving as photocatalyst carrier or promoter.^[4] Commonly, under solar irradiation, those aligned vessel micro/nano-channels can continuous transport water via the upward vapor flow which benefit the contact between photocatalysts and pollutants.^[5] Meanwhile, the abundant lignin content in wood block can serve as an effective agent to reduce metal ions to metal NPs.^[4a] Therefore, wood carbon is an ideal supporting material for visible light driven photocatalysts.

Herein, we proposed a ternary nano-photocatalysts hybridized plasmonic 3D wood carbon by in situ forming and decorating Pt/Au/TiO₂ NPs into a natural wood matrix by a simple two-step calcination method for high efficiency photodegradation of Tetracycline. Plasmonic resonances near the surface of the Pt/Au NPs would suppress the reorganization of photogenerated electron-hole pairs in TiO₂ and produce an enhancement of photocatalytic process. Meanwhile, the effective photothermal effect of wood carbon facilitates the interfacial steam evaporation process and accelerates the upward diffusion of contaminants toward the floating composites, which enhances further the photodegradation rate and efficiency of TC.

Results and Discussion

The precursor wood piece is derived directly from the natural wood in trees, for its abundant open and aligned microchannels which can pump water owing to its transpiration ability.^[4b] Meanwhile, the natural porous structure is an ideal host for loading of ternary Pt/Au/TiO₂ NPs, as shown by scanning electron microscopy (SEM) in Figure S1. The wood carbon was obtained by direct calcination of a piece of preformed TiO₂-decorated wood block under N₂ condition and the similar Raman spectrum (Figure S2) intensity of D peak and G peak confirm its amorphous feature, which is similar to other reported hard carbon materials.^[6] The ternary Pt/Au/TiO₂ NPs-decorated wood carbon with a final mean NP size of ~ 500 nm was then prepared in-situ by a simple chemical and calcination method to grow Pt/Au nano-components on the preformed TiO₂/wood carbon. The detailed preparation method was shown in experiment section. The element distribution of C, Ti, O, Au and Pt atoms was studied by SEM and its mapping images were shown in Figure 1a-f. Meanwhile, the EDX line scan profile (Figure 1g) revealed that Pt and Au atoms, though not heavily, were both homogeneously distributed throughout the preformed TiO₂ NPs to form ternary composite NPs, rather than the

[a] M. M. Wang, Dr. P. Wang, Dr. J. Zhang, C. P. Li, Prof. Y. D. Jin. State Key Laboratory of Electroanalytical Chemistry, Changchun Institute of Applied Chemistry, Chinese Academy of Sciences, Changchun 130022, Jilin, China.

[b] M. M. Wang, C. P. Li, Prof. Y. D. Jin. University of Chinese Academy of Sciences, Beijing 100049, China. Email: ydj@ciac.ac.cn

Supporting information for this article is given via a link at the end of the document.

formation of individual Au and Pt NPs.

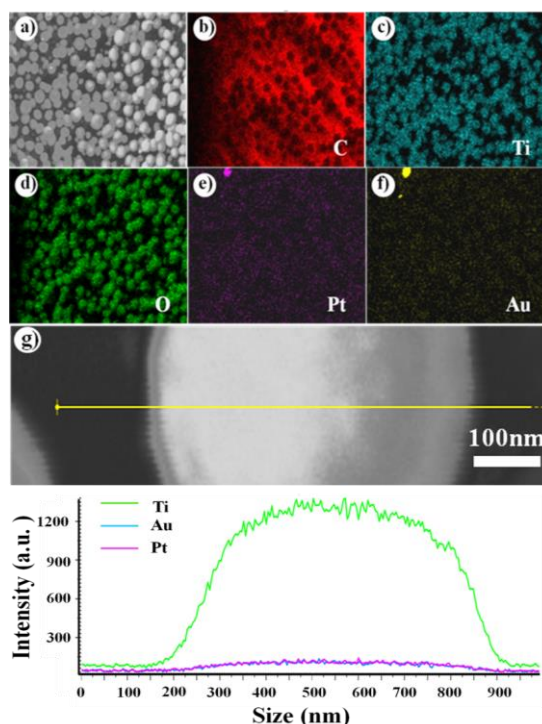


Figure 1. (a-f) SEM image and corresponding element mapping images of the as-prepared Pt/Au/TiO₂ NPs on the microchannels of wood carbon. (g) EDX line scan profiles of a Pt/Au/TiO₂ NP.

To further verify the ternary heterogeneous structure of the as-prepared Pt/Au/TiO₂ NPs, the prepared samples were characterized by UV-vis spectra. As shown in Figure 2a, TiO₂ NPs absorb in ultraviolet zone with a wavelength range of 200–350 nm, while the ternary Pt/Au/TiO₂ NPs have a broad plasmonic absorption band in the visible and near infrared region for the deposition of plasmonic Au component, which demonstrates the formation of Pt/Au/TiO₂ hybrid nanostructures. The phase structures of the as-prepared samples were investigated by X-ray diffraction pattern and the results were shown in Figure 2b. Both the as-prepared TiO₂ and the resulting ternary Pt/Au/TiO₂ NPs can be well indexed to tetragonal rutile (JCPDS No. 21-1276).^[7] In addition, XRD peaks corresponding to AuNPs (JCPDS No. 04-0784) are observed in the Pt/Au/TiO₂ samples which confirmed the successful reduction of Au over the TiO₂. X-ray photoelectron spectroscopy (XPS) analyses were further performed to identify the elemental state of the Pt/Au/TiO₂ catalysts. Figure 2c shows the Ti, Au and Pt XPS spectra of the as-prepared Pt/Au/TiO₂ NPs. The binding energy for Ti 2p_{3/2} and Ti 2p_{1/2} at 458 and 463 eV, respectively, asserts the existence of Ti⁴⁺ state.^[8] While the orbitals of Au 4f_{7/2}, Au 4f_{5/2} and Pt 4f_{5/2} are located at 82.6, 86.1 and 73.4 eV, suggesting that both Au and Pt are presented in metallic state.^[9] It further confirmed the formation of Pt and Au nanocomponents on the surface of TiO₂.

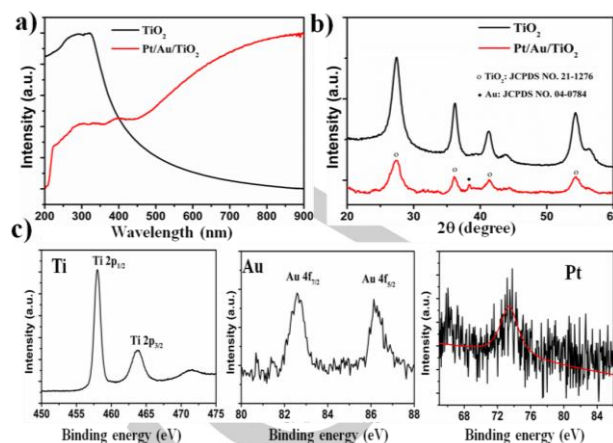


Figure 2. (a) UV-vis spectra of TiO₂ and ternary Pt/Au/TiO₂ NPs. (b) XRD patterns of the TiO₂ and Pt/Au/TiO₂ NPs. (c) XPS spectra of Ti 2p, Au 4f, and Pt 4f of the as-prepared Pt/Au/TiO₂ NPs.

Furthermore, the as-prepared Pt/Au/TiO₂-wood carbon was highly hydrophilic as shown in Figure S3a, which is conducive to transport water upwards and maintain a continuous water supply for the vapor generation. More importantly, the as-prepared hydrophilic plasmonic wood carbon can float on water for its natural microchannels structure (Figure S3b), which benefits to minimize the heat loss and enhances steam generation efficiency via the efficient interfacial water heating. As shown in Figure S4, the 2.5 mm-thick TiO₂-wood carbon and Pt/Au/TiO₂-wood carbon displayed almost full absorption in a wide wavelength range from 200 nm to 2500 nm. Figure 3a shows the thermal images of the TiO₂-wood carbon and Pt/Au/TiO₂-wood carbon based floating system recorded at the same illumination intensity and time (using an infrared camera), revealing that the Pt/Au/TiO₂-wood carbon is a better heat generator with an extremely high solar vapor generation efficiency up to 90.4% achieved at 10 kW m⁻², which was higher than that of TiO₂-wood carbon (75.3%) as shown in Figure 3b. The vapor generation efficiency was calculated by the formula of $\eta = \dot{m} h_{LV} / I$,^[9a] in which \dot{m} is the mass flux, h_{LV} denotes the total enthalpy of the sensible heat and liquid-vapor phase change, and I is the power density of light irradiation. Although the as-prepared Pt/Au/TiO₂-wood carbon did not show the best solar vapor generation efficiency compared to previous reports.^[9a,10] The facile fabrication and good mechanical property of the plasmonic wood carbon make it promising for sustainable clean water generation applications.

The utilization of renewable solar energy for catalysis and treatment of polluted water is envisioned a sustainable route for increasing clean energy and water supplies. Such excellent interfacial solar steam generation performance of the floating system will benefit for mass transport and photodegradation of water pollutants. We then exploited the ternary Pt/Au/TiO₂ NPs-decorated wood carbon as floating plasmonic catalysts for photodegradation of TC. TC is one of the most used antibiotics

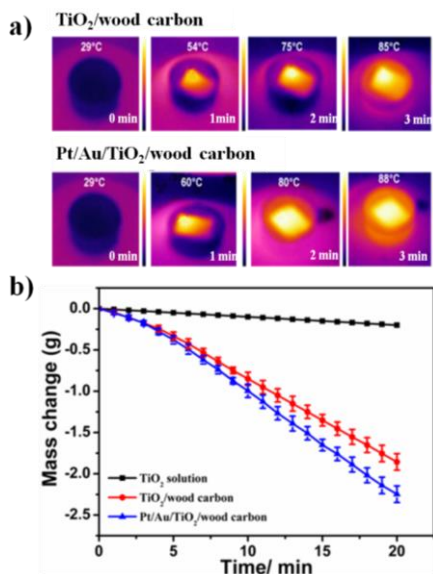


Figure 3. (a) IR pictures of TiO₂/wood carbon and Pt/Au/TiO₂-wood carbon at the same illumination time. (b) Mass changes over time through steam generation under solar irradiation at 10 kW m⁻².

in veterinary medicine by some intensive farming operations and it can exist persistent in soils and water, which is very harmful to human being.^[2,11] Therefore, it is highly desired to explore efficient and environment-friendly photocatalysts to remove TC from the polluted water. Before photocatalytic performance test, a slice of the catalyst-supported wood carbon was placed floating on a TC solution ($C_0=40$ mg L⁻¹) and kept in dark for ~30 min to reach absorption-desorption balance. The photocatalytic activity, i.e. the degradation rate of TC, was evaluated by monitoring its characteristic absorption bands at 275 nm and 357 nm under visible light illumination ($\lambda>420$ nm). As clearly shown in Figure 4a, the TC concentration did not decrease over time without the catalysts after continued visible light irradiation, which excludes its self-photolysis process. Meanwhile, for the prepared TiO₂ mono-catalysts, there is no apparent photodegradation performance after 80 min visible light irradiation. Impressively, the degradation of TC was remarkably accelerated with the floating Pt/Au/TiO₂-wood carbon as catalysts ($k=2.9\times10^{-2}$ min⁻¹); it can degrade 94% of TC in 80 min, which was higher than the TiO₂/wood carbon catalyst (81%, with $k=1.7\times10^{-2}$ min⁻¹) and it is also superior to the previously reported photocatalysts (Table 1). We should note that the degradation efficiency in Table 1 was obtained by calculating TC photodegradation rate under unit catalyst and unit time. As a comparison, the content of TC also decreased ~20% for the Pt/Au/TiO₂-wood carbon photocatalyst under dark condition for 110 min (Figure S5), which may be caused by the high adsorption capacity of wood carbon. The phenomena directly indicated that the wood carbon serving as photocatalyst carrier can effectively promote the photocatalytic degradation of TC. Meanwhile, the introduction of Pt and Au nanocomponents on TiO₂ can effectively improve the electron-hole pair separation for its Schottky contact. The kinetic curves shown in Figure 4b

indicates a first-order reaction of the photocatalytic process for the as-prepared catalysts. We also examined the performances of Pt/Au/TiO₂-wood carbon for the solar steam generation and photodegradation of TC under lower light densities (Figure S6). Under light irradiation at 2 kW m⁻² intensity for 80 min, the vapor generation efficiency of the system reached ~73% (Figure S6a), while the photodegradation rate of TC was up to ~82% (Figure S6b). Control experiments using binary photocatalysts of Au/TiO₂-wood carbon, Pt/TiO₂-wood carbon and ternary Pt/Au/TiO₂-wood carbon were also performed. As shown in Figure S7, the ternary Pt/Au/TiO₂-wood carbon catalyst exhibited the best photocatalytic performance, which demonstrates that both Au and Pt nanocomponents play important roles in the photodegradation of TC.

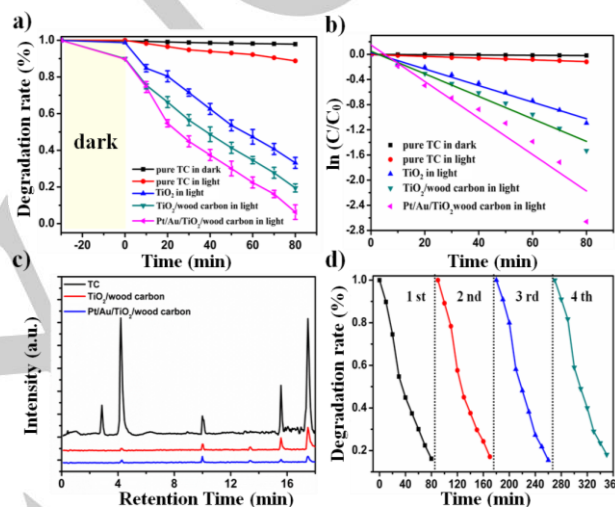


Figure 4. (a) Photocatalytic degradation efficiency of TC (40 mg L⁻¹) under visible light irradiation over TiO₂, TiO₂/wood carbon and Pt/Au/TiO₂-wood carbon, under the same concentration of catalyst used (0.1 g L⁻¹). (b) Kinetic curves for TC degradation over as-prepared photocatalysts. (c) HPLC-MS chromatograms of TC without and with degradation over TiO₂/wood carbon and Pt/Au/TiO₂-wood carbon under visible-light irradiation for 80 min. (d) Cycling runs for degradation efficiency over Pt/Au/TiO₂-wood carbon photocatalysts under visible light irradiation.

High performance liquid chromatography-mass spectrometry (HPLC-MS) was further employed to identify the photocatalytic reaction products of the system. As shown in Figure 4c, the TC peak eluted at a retention time of ~4.28 min decreased largely after 80 min visible light irradiation in the presence of photocatalyst of TiO₂-wood carbon or Pt/Au/TiO₂-wood carbon. The product of m/z (mass-to-charge ratio) at 410 eluted at a retention time of 4.28 min was attributed to the detaching of NH₃ and H₂O from TC (Figure S8a). The most intense daughter ion with m/z of 410 was selected for the quantification of TC photodegradation in our system.^[12] The intensity of TC (m/z 410) peak decreased largely after 80 min visible light irradiation both for the photocatalyst of TiO₂-wood carbon and Pt/Au/TiO₂-wood carbon. Meanwhile, some intermediates with m/z at 302, 284, 252, 198 and 140 were generated. These results demonstrated that TC was photo-degraded with time.^[13] As shown in Figure

S8b and Figure S8c, the Pt/Au/TiO₂-wood carbon photocatalyst exhibited the highest TC degradation rate under the same conditions. The proposed photocatalytic degradation pathway of TC over the as-prepared Pt/Au/TiO₂-wood carbon is shown in Figure S9. Meanwhile, as shown in Figure S10, the solution total organic carbon (TOC) removal reached to 71% after 160 min photocatalysis over the as-prepared Pt/Au/TiO₂-wood carbon, indicating that TC was gradually photodegraded to CO₂ and water. As a result, as shown in the HPLC-MS spectra (Figure S8), both the intensity of TC and its intermediates were decreased correspondingly during the photolysis process. The stability of the as-prepared Pt/Au/TiO₂-wood carbon was also investigated. As clearly shown in Figure 4d, there is no apparent decrease in the photocatalytic performance even after four consecutive cycles, which demonstrates that the as-prepared Pt/Au/TiO₂-wood carbon floating photocatalysts own high catalytic stability and good performance for photodegradation of TC.

Table 1. Photocatalytic activity of Pt/Au/TiO₂-wood carbon compared to previously reported photocatalysts.

Reference	Materials	Photocatalysts mass (mg)	TC content (mg)	Degradation efficiency (×10 ⁻² ·h)
Appl. Catal. B: Environ. 186 (2016) 19-29	In ₂ S ₃ @MIL-125(Ti)	40	4.6	7.27
Appl. Catal. B: Environ. 201 (2017) 617-628	g-C ₃ N ₄ /K ⁺ Ca ₂ Nb ₃ O ₁₀ ⁻ nanosheet	40	1.4	1.89
Appl. Catal. B: Environ. 229 (2018) 96-104	carbon dots modified MoO ₃ /g-C ₃ N ₄	30	1	1.96
Appl. Catal. B: Environ. 164 (2015) 297-304	Ag/AgBr/AgIn(MoO ₄) ₂	100	1	0.7
ACS Appl. Mater. Interfaces 8(2016) 32887-32900	AgI (20wt %)/BiVO ₄	30	2	6.3
Appl. Catal. B: Environ. 209 (2017) 720-728	Z-scheme Ag ₃ PO ₄ /CuBi ₂ O ₄	50	1	1.4
This work	Floating Pt/Au/TiO₂-wood carbon	10	4	14

To provide a mechanistic insight into the photocatalytic process, EDTA and isopropanol (IPA) were used to demonstrate

the roles of h⁺ and ·OH in the TC photodegradation process.^[1c, 14] As shown in Figure 5a, when 1 mmol of IPA and 1 mmol of EDTA-2Na were added into the photocatalytic system, the degradation efficiency of TC was both decreased, which suggests that both h⁺ and ·OH played important roles towards TC photodegradation. Therefore, as schematically illustrated in Figure 5b, upon illumination of the hybrid system, the electrons in VB of TiO₂ can be photo-excited to the CB, leaving holes in the VB of TiO₂; the photo-excited holes stay in the VB of TiO₂ to directly oxidize OH⁻ to form ·OH active species. Meanwhile, the electrons are capable of capture by plasmonic hot holes photo-generated by the Pt/Au nanocomponents for its strong electron oscillation collectively on the LSPR excitation, which effectively suppress the recombination of photogenerated electrons and holes of TiO₂ and hence enhance the photocatalytic performance of the system. Meanwhile, the photo-excited electrons can be quickly transferred to Pt through metal-semiconductor interfaces. And then the electrons are trapped by Pt and consumed by reduction reaction. Consequently, the recombination of electrons and holes is suppressed.^[15] Besides this, another plasmonic effect, via interfacial photothermal steam generation, are considered to accelerate the upward diffusion of contaminants toward the floating membrane composites and further enhance the photocatalytic performance of TC degradation.

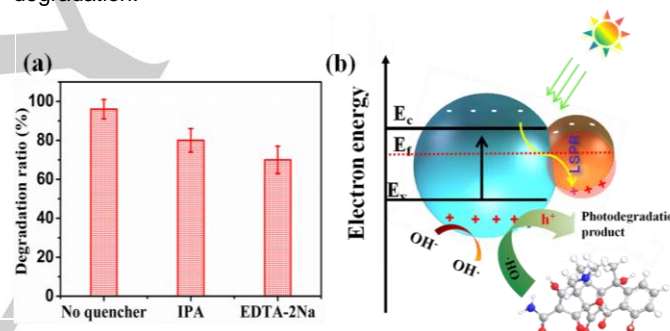


Figure 5 (a) Trapping experiment of active species during the photocatalytic reaction. (b) Schematic illustration of photo-generated charge carrier's separation and transfer in the Pt/Au/TiO₂ hybrid nanostructure.

Conclusions

In summary, we report herein an effective photocatalytic water purification system based on ternary Pt/Au/TiO₂ NPs-decorated plasmonic wood carbon and exploit it for highly effective photodegradation of TC. As experimentally demonstrated, the plasmonic property of the fine metal nanoparticles make great contribution to the photodegradation rate of TC at visible light condition. What's more, the plasmonic wood carbon as a high solar absorbent has high solar steam generation efficiency which can accelerate the upward diffusion of contaminants toward the floating membrane composites. Meanwhile, the unique floating structure makes it convenient for potential recycling use. Such recyclable solar evaporation-assisted photodegradation floating device is envisioned very promising for practical versatile clean water regeneration applications.

Experimental Section

Materials and Chemicals. The basswood used in our experiments was from Walnut Hollow Company, Potassium platinum(IV) chloride (K_2PtCl_6 , $\geq 99.0\%$), and chloroauric (IV) acid ($HAuCl_4 \cdot 3H_2O$) were purchased from Sigma-Aldrich. Titanium tetrachloride (98%) was purchased from Beijing Chemical Works.

Preparation of TiO_2 /wood carbon blocks. TiO_2 nanoparticles was prepared according to previous method.^[16] Typically, titanium tetrachloride was dropped into ethanol under stirring and the mixture solution was stirred for several minutes at room conditions, and then, a sol with transparent yellowish was formed. Finally, a mount of distilled water was added slowly under stirring. In our system, the molar ratios of $TiCl_4$, ethanol and water was 2:20:280. Then a piece of wood block (2.5 mm in thickness) was immersed in to the above solution, and vacuum processing till the wood block sink to bottom of solution, and then the system was maintained in a vacuum state at 50 °C for 24 h. The TiO_2 /wood block was obtained by several times water washing to remove the surface TiO_2 and make pH of the block to neutral. Finally, the as-prepared dried TiO_2 /wood block was calcinated at 750°C under Ar condition for 2 h.

Preparation of Pt/Au/ TiO_2 -wood carbon blocks. A piece of the as-prepared TiO_2 /wood block was immersed into the mixture potassium platinum (IV) chloride (0.01%) and chloroauric (IV) acid (0.01%) aqueous solution for 12 h at 25 °C and then calcinated at 750°C under Ar condition for 2 h. And finally the plasmonic Pt/Au/ TiO_2 -wood carbon block was obtained.

Characterizations. A Cary 500 Scan UV-vis spectrophotometer (Varian, U.S.A.) was used to measure the UV-Vis absorption spectra. A Hitachi S4800 field emission scanning electron microscope (SEM) equipped with an energy dispersive spectrometer was used to determine the detailed microstructure. We study the crystal structure of the as-prepared samples by wide-angle X-ray diffraction (XRD, D8 ADVANCE, Germany BRUKER company) with a Cu target. The electronic structure was analysed by X-ray photoelectron spectroscopy (Escalab 250Xi, Thermo Fisher Scientific). A Xeon lamp (300 W) equipped with the filter of $\lambda > 420$ nm (10 kW m⁻²) was used as the light source. The photocatalyst products were analysed by a high performance liquid chromatography-mass spectrometry (HPLC-MS) system equipped with a Waters BEH-C18 column (50×2.1 mm, 1.7 μ m). The mobile phase was acetonitrile with 0.1% Formic acid and water with a flow rate of 0.3 ml min⁻¹ and the column temperature was room temperature.

Experiments for photocatalysis of TC. We put the as-prepared plasmonic wood blocks in a glass chamber filled with 50 ml TC (40 mg L⁻¹) water. The mass of the photocatalyst was 10 mg and it was obtained by calculating the weight change of wood blocks before and after nanoparticle modification. A Xeon lamp (300 W) equipped with the filter of $\lambda > 420$ nm was used in illumination experiments. We record the mass change by an electronic balance (accuracy: 0.1 mg) to accurately measure the evaporation rates. The irradiated area on the plasmonic wood carbon block was approximately 6.25 cm². The absorbance of TC solution was Measured every ten minutes by UV-vis absorption spectra. Simultaneously, we record the surface temperature of the plasmonic wood block by infrared camera.

Acknowledgements

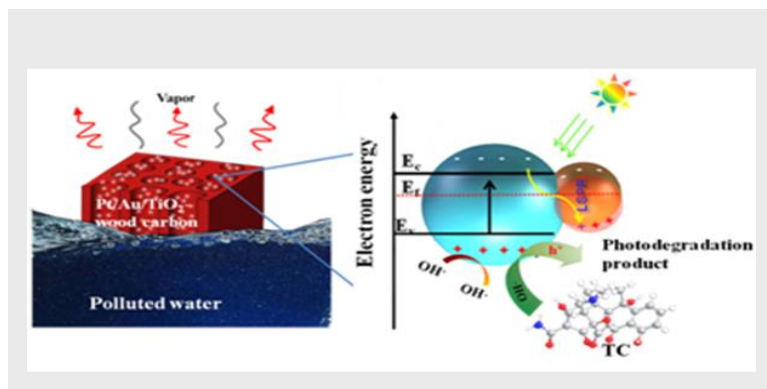
This work was financially supported by the National Natural Science Foundation of China (Grant Nos. 21475125, 21175125, 51502286), the Hundred Talents Program of the Chinese Academy of Sciences, and the State Key Laboratory of Electroanalytical Chemistry (no. 110000R387).

Keywords: solar energy • Pt/Au/ TiO_2 -wood carbon • plasmonic • solar evaporation • photocatalytic

- [1] a) H. Zhu, W. Luo, P. N. Ciesielski, Z. Fang, J. Y. Zhu, G. Henriksson, M. E. Himmel, L. Hu, *Chem. Rev.* **2016**, 116, 9305-9374; b) Y. Yang, R. Zhao, T. Zhang, K. Zhao, P. Xiao, Y. Ma, P. M. Ajayan, G. Shi, Y. Chen, *ACS Nano* **2018**, 1, 829-835; c) X. Yan, X. Wang, W. Gu, M. Wu, Y. Yan, B. Hu, G. Che, D. Han, J. Yang, W. Fan, W. Shi, *Appl. Catal. B: Environ.* **2015**, 164, 297-304.
- [2] B. Luo, D. Xu, D. Li, G. Wu, M. Wu, W. Shi, M. Chen, *ACS Appl. Mater. Inter.* **2015**, 7, 17061-17069.
- [3] a) Y. Yang, E. Liu, H. Dai, L. Kang, H. Wu, J. Fan, X. Hu, H. Liu, *Inter. J. Hydrogen Energy* **2014**, 39, 7664-7671; b) Q. Zhang, D. Q. Lima, I. Lee, F. Zaera, M. Chi, Y. Yin, *Angew. Chem. Inter. Ed.* **2011**, 50, 7088-7092; c) S. Naya, A. Inoue, H. Tada, *J. Am. Chem. Soc.* **2010**, 132, 6292-6293.
- [4] a) M. Zhu, Y. Li, F. Chen, X. Zhu, J. Dai, Y. Li, Z. Yang, X. Yan, J. Song, Y. Wang, E. Hitz, W. Luo, M. Lu, B. Yang, L. Hu, *Adv. Energy Mater.* **2017**, 1701028; b) F. Chen, A. S. Gong, M. Zhu, G. Chen, S. D. Lacey, F. Jiang, Y. Li, Y. Wang, J. Dai, Y. Yao, J. Song, B. Liu, K. Fu, S. Das, L. Hu, *ACS Nano* **2017**, 11, 4275-4282.
- [5] a) G. Xue, K. Liu, Q. Chen, P. Yang, J. Li, T. Ding, J. Duan, B. Qi, J. Zhou, *ACS Appl. Mater. Inter.* **2017**, 9, 15052-15057; b) K. K. Liu, Q. Jiang, S. Tadepalli, R. Raliya, P. Biswas, R. R. Naik, S. Singamaneni, *ACS Appl. Mater. Inter.* **2017**, 9, 7675-7681.
- [6] C. Chen, Y. Zhang, Y. Li, J. Dai, J. Song, Y. Yao, Y. Gong, I. Kierzewski, J. Xie, L. Hu, *Energy Environ. Sci.* **2017**, 10, 538-545.
- [7] Y. W. Wang, L. Z. Zhang, K. J. Deng, X. Y. Chen, Z. G. Zou, *J. Phys. Chem. C* **2007**, 111, 2709-2714.
- [8] H. Wang, X. Yuan, Y. Wu, G. Zeng, H. Dong, X. Chen, L. Leng, Z. Wu, L. Peng, *Appl. Catalysis B: Environ.* **2016**, 186, 19-29.
- [9] a) M. M. Wang, J. Zhang, P. Wang, C. P. Li, X. L. Xu, Y. D. Jin, *Nano Res.* **2018**, 11, 3854-3863. b) K. Tang, X. F. Wang, Q. Li, C. L. Yan, *Adv. Mater.* **2018**, 30, 1704779.
- [10] a) Q. M. Chen, Z. Q. Pei, Y. S. Xu, Z. Li, Y. Yang, Y. Wei, Y. Ji, *Chem. Sci.* **2018**, 9, 623-628; b) X. D. Yang, Y. B. Yang, L. N. Fu, M. C. Zou, Z. H. Li, A. Y. Cao, Q. Yuan, *Adv. Funct. Mater.* **2018**, 28, 1704505.
- [11] a) D. Jiang, T. Wang, Q. Xu, D. Li, S. Meng, M. Chen, *Appl. Catalysis B: Environ.* **2017**, 201, 617-628. b) X. L. Wang, Q. Liu, Q. Yang, Z. G. Zhang, X. M. Fang, *Carbon* **2018**, 136, 103-112.
- [12] D. Debayle, G. Dessalces, M. F. Grenier-Loustalot, *Anal. Bioanal. Chem.* **2008**, 391, 1011-1020.
- [13] a) X. L. Liu, P. Lv, G. X. Yao, C. C. Ma, P. W. Huo, Y. S. Yan, *Chem. Eng. J.* **2013**, 217, 398-406; b) J. F. Niu, S. Y. Ding, L. W. Zhang, J. B. Zhao, C. H. Feng, *Chemosphere* **2013**, 93, 1-8.
- [14] W. Wang, J. Fang, S. Shao, M. Lai, C. Lu, *Appl. Catalysis B: Environ.* **2017**, 217, 57-64.
- [15] J. J. Zou, C. Chen, C. J. Liu, Y. P. Zhang, Y. Han, L. Cui, *Mater. Letters*, **2005**, 59, 3437-3440.
- [16] Y. W. Wang, L. Z. Zhang, K. J. Deng, X. Y. Chen, Z. G. Zou, *J. Phys. Chem. C* **2007**, 111, 2709-2714.

Layout 2:

FULL PAPER



Minmin Wang,^{[a],[b]} Ping Wang,^[a] Jie Zhang,^[a] Chuanping Li,^{[a],[b]} and Yongdong Jin^{*[a],[b]}

Page No. – Page No.

Ternary Pt/Au/TiO₂-Decorated Plasmonic Wood Carbon for High-Efficiency Interfacial Solar Steam Generation and Photodegradation of Tetracycline

A ternary Pt/Au/TiO₂ decorated plasmonic wood carbon based floating device was explored for photodegradation of tetracycline. The effective solar steam evaporation capability benefits for the contact and mass transfer of contaminants with the catalysts. Meanwhile, plasmonic effect of Pt/Au NPs promotes charge separation over TiO₂. A high photodegradation rate of TC (at 40 mg L⁻¹) up to 94% after 80 min continuous light irradiation ($\lambda > 420$ nm) was achieved, which is superior to previously reported photocatalysts.